INFECTION AND IMMUNITY, Sept. 2011, p. 3810–3820 Vol. 79, No. 9
0019-9567/11/$12.00 doi:10.1128/IAI.00051-11

Identification of a Novel Virulence Factor in *Clostridium Difficile* That Modulates Toxin Sensitivity of Cultured Epithelial Cells[▽]

Masashi Miura,[1]* Haru Kato,[2] and Osamu Matsushita[3]

Department of Foodborne Infection Research (SRL, Inc.), Kitasato University School of Medicine, Kanagawa, Japan[1]; Department of Bacteriology II, National Institute of Infectious Diseases, Tokyo, Japan[2]; and Department of Microbiology, Kitasato University School of Medicine, Kanagawa, Japan[3]

Received 13 January 2011/Returned for modification 13 February 2011/Accepted 29 June 2011

Two glucosylating toxins named toxins A and B play a role in the pathogenesis of *Clostridium difficile* infection. The interaction of the toxins with host cell factors proceeds to downstream stages of cytotoxic effects in cells, in which involvement of other *C. difficile* factors remains unknown. We utilized culture filtrate of *C. difficile* with a low dilution to characterize the influence of putative minor proteins on the organization of the actin cytoskeleton in cultured epithelial cells and found a previously uncharacterized F-actin aggregated structure, termed "actin aggregate," at the juxtanuclear region. We reasoned that formation of actin aggregate was due to an additional factor(s) in the culture filtrate rather than the glucosylating toxins, because treatment of purified toxins rarely caused actin aggregate in cells. We focused on a previously uncharacterized hypothetical protein harboring a KDEL-like sequence as a candidate. The product of the candidate gene was detected in culture filtrate of *C. difficile* ATCC 9689 and was renamed Srl. Purified glutathione *S*-transferase-tagged Srl triggered formation of actin aggregate in the cells in the presence of either toxin A or B and enhanced cytotoxicity of each of the two toxins, including decreases in both cell viability and transepithelial resistance of cultured epithelial monolayer, although the recombinant Srl alone did not show detectable cytotoxicity. Srl-neutralized culture filtrate partially inhibited morphological changes of the cells in parallel with decreased actin aggregate formation in the cells. Thus, Srl might contribute to the modulation of toxin sensitivity of intestinal epithelial cells by enhancing cytotoxicity of *C. difficile* toxins.

Clostridium difficile, a Gram-positive spore-forming, anaerobic bacterium, is the causative agent of almost all cases of pseudomembranous colitis as well as many cases of antibiotic-associated diarrhea (3, 13). Its pathogenicity is mediated mainly by two exotoxins, TcdA (toxin A) and TcdB (toxin B). These two toxins share more than 60% amino acid sequence homology and damage the human colonic mucosa (36). The majority of toxigenic *C. difficile* strains produce both toxins A and B (toxigenic type A^+ B^+), whereas a minority exclusively produce toxin B (toxigenic type A^- B^+) due to a deletion in the *tcdA* (toxin A) gene (41). Recent studies using mutagenesis techniques have revealed that toxin B is a key virulence determinant of *C. difficile* and reestablished that both toxin A and toxin B are important factors of virulence (26, 30).

Inside the cell, toxins monoglucosylate, thereby inactivating low-molecular-weight Rho subfamily GTPases. On cultured intestinal epithelial cells, the cytotoxic effect is characterized by a reduction in transepithelial resistance (TER), indicating a loss of the barrier function of intestinal tight junctions. Rho glucosylation of cultured cells results in the disappearance of polymerized filamentous actin (F-actin), peripheral membrane ruffling, and finally the complete loss of the cell shape into cell rounding termed the "cytopathic effect." The toxins also provoke mitochondrial damage that eventually proceeds to apoptosis (2, 5, 12, 14, 17, 31, 35, 40).

Recent studies have focused on virulence or virulence-associated factors other than toxins A and B that might also be involved in the pathogenesis of *C. difficile*. Some toxigenic *C. difficile* strains produce an actin ADP-ribosylating toxin called "*C. difficile* toxin" (CDT). Putative colonization factors such as surface layer proteins (SLPs), Cwp66 adhesins, and Cwp84 protease have been characterized (18, 21, 22, 24, 42). However, no study has focused on toxin A- or toxin B-associated virulence factors that could modulate their cytopathic effects.

Studies have previously investigated the structural changes of cellular organelles in relation to toxin-induced cytopathic effects (39). Partially purified toxin B causes loss of fibronectin from the surfaces of cells, paralleling the appearance of the cytopathic effect (1). It also causes the condensation of actin in the perinuclear region of mast cells (32). On the other hand, *C. difficile* toxin A induces microtubule instability and disorganization of focal adhesions (23, 34). In the present study, we further characterized cytoskeletal rearrangement associated with the cytopathic effect in cells by *C. difficile* toxins in culture filtrate and found F-actin aggregation in the juxtanuclear Golgi region, due to an enhanced cytoskeletal rearrangement by unknown factors. We identified a novel virulence-associated factor, Srl, that appears to be responsible for this observable effect. As Srl might play a role in modulating toxin sensitivity of intestinal epithelial cells by enhancing cytotoxicity of *C. difficile* toxins A and B, we have called the factor "Srl" (for *s*ensitivity *r*egu*l*ation of *C. difficile* toxins).

* Corresponding author. Mailing address: Department of Foodborne Infection Research (SRL, Inc.), Kitasato University School of Medicine, 1-15-1 Sagamihara-shi, Minami-ku, Kanagawa 252-0374, Japan. Phone: 81-42-778-9350. Fax: 81-42-778-9355. E-mail: miuram@med.kitasato-u.ac.jp.

▽ Published ahead of print on 11 July 2011.

MATERIALS AND METHODS

Antibody, reagent, and strains. The following materials were obtained from Invitrogen unless otherwise noted: tetramethyl rhodamine isothiocyanate-conjugated phalloidin (TRITC-phalloidin), Alexa Fluor 488-conjugated phalloidin (Alexa 488-phalloidin), 4′,6-diamino-2-phenylindole (DAPI), goat anti-rabbit secondary antibody conjugated to Alexa Fluor 488, goat anti-rabbit secondary antibody conjugated to Texas Red, and goat anti-mouse secondary antibody conjugated to Texas Red. The following materials were obtained from the indicated suppliers: monoclonal anti-Golgi region 58,000-molecular-weight (58K) protein antibody (Abcam), goat anti-rabbit secondary antibodies conjugated to horseradish peroxidase (Bio-Rad), and purified toxins A and B (Sigma) (7, 29). The plasmid encoding the green fluorescent protein (GFP)-fused C-terminal actin-binding domain of human moesin (pGFP-Cterm-moesin) was provided by H. Watanabe. Rabbit polyclonal anti-Srl antibodies were raised against a synthetic peptide (KLDKFDEVLEEKNLTKKEWLEEKIDEELEQ) corresponding to C-terminal regions of Srl and affinity purified using an IgG purification kit (Pierce). *C. difficile* strain ATCC 9689 (toxigenic type A^+ B^+, toxinotype 0, *cdtA* negative (4) and *Clostridium novyi* strain ATCC 17861 were obtained from the Japan Collection of Microorganisms (Riken BioResource). Twenty-six *C. difficile* clinical isolates collected in Japan were used in this study.

Cloning and sequencing of *srl* gene. A 541-bp PCR product was amplified from ATCC 9689 genomic DNA using upstream (5′-GGAATGTAAATTGC TGTGATTTCAC-3′) and downstream (5′-CATAATATTACACTCCTTAA TAATTG-3′) primers, which were used as templates for DNA sequencing. The *srl* encoding the protein from amino acid 1 to amino acid 62 was amplified by PCR from ATCC 9689 genomic DNA with appropriate primers, adding an EcoRI site at the 5′ end and a SalI site at the 3′ end, followed by cloning into pGEX-4T-1 (GE Healthcare) and sequencing for confirmation, resulting in plasmid pGST-Srl.

TCA precipitation of culture filtrate, Western blotting, and enzyme immunoassays. For assays of Srl production, ATCC 9689, ATCC 17861, and clinical isolates of *C. difficile* were grown in 10 ml of Gifu anaerobic medium (GAM) broth for 3 days at 37°C. The samples were centrifuged at 14,000 × *g* for 2 min to give the bacterial pellet and supernatant fraction. The bacterial pellet was solubilized in SDS-PAGE sample buffer, boiled for 5 min, and subjected to SDS-PAGE. The supernatant was passed through a 0.2-μm-pore-size membrane filter resulting in the culture filtrate, and proteins in the filtrate were precipitated with 6% trichloroacetic acid (TCA). The precipitates were washed with acetone and solubilized in SDS sample buffer, boiled for 5 min, and subjected to 20% SDS-PAGE and silver staining or Western blotting using anti-Srl antibody. Western blot detection was carried out with the ECL kit (Perkin Elmer). For detection of toxins A and B among clinical isolates of *C. difficile*, a Tox A/B Quik Chek (Nissui) test was performed according to the manufacturer's instructions.

Purification of GST-Srl. The Srl protein containing an N-terminal glutathione *S*-transferase (GST) tag was expressed in *Escherichia coli* BL21 (Novagen) harboring pGST-Srl. Purification was performed using Sepharose 4B affinity resin (GE Healthcare) according to the manufacturer's recommendations. The eluted recombinant protein was dialyzed to phosphate-buffered saline and analyzed by 12.5% SDS-PAGE and Coomassie brilliant blue (CBB) staining or Western blotting using anti-Srl antibody.

Observations of actin aggregate. MDCK cells cultured in Dulbecco's modified Eagle medium (DMEM) containing 10% heat-inactivated fetal bovine serum were seeded on coverslips at 6×10^4 cells per well in 24-well plates and incubated for 24 h. Caco-2 cells cultured in minimal essential medium containing 10% heat-inactivated fetal bovine serum and 1% nonessential amino acids (DS Pharma Biomedical) were seeded on coverslips at 6×10^4 cells per well in 24-well plates and incubated for 7 days. To prepare the culture filtrate, *C. difficile* was grown in 10 ml of GAM broth for 3 days at 37°C, and the culture filtrate was obtained by centrifugation following filter sterilization as described above. To limit effects from the GAM broth itself, a modified low-dilution technique using the culture filtrate was applied (9). Briefly, a 3-fold dilution of the culture filtrate in DMEM was added to the cells. After a 30-min exposure, cells were replaced with DMEM, further incubated for 3 h, and fixed with 3.7% paraformaldehyde followed by TRITC-phalloidin plus DAPI labeling for observation by fluorescence microscopy (Nikon Eclipse E400 system). For monitoring F-actin cytoskeleton dynamics in living cells, MDCK cells were seeded at 6×10^4 cells in 35-mm glass-bottomed dishes (Matsunami) and incubated for 24 h. The dishes were transiently transfected with the pGFP-Cterm-moesin plasmid using Lipofectamine 2000 reagent (Invitrogen) according to the manufacturer's instructions. After 48 h of transfection, the culture medium was removed, after which cells were washed with serum-free medium. Transfectants were treated with a 3-fold dilution of *C. difficile* culture filtrate, 850 ng/ml toxin A, or 400 ng/ml toxin B in 3-fold dilutions of bacterium-free culture medium for 30 min. The medium was replaced with DMEM and monitored for 3 h by a live imaging system (Nikon BioStation IM). Then, cells were fixed and immunolabeled with anti-Golgi region 58K protein antibody. For GST-Srl treatment, MDCK or Caco-2 cells were treated with 10 μg/ml GST-Srl or GST (plus either 750 ng/ml toxin A or 300 ng/ml toxin B) and incubated at 37°C for 3 h or 24 h. To wash off GST-Srl, the medium containing GST-Srl was removed, after which cells were washed with serum-free medium and then 750 ng/ml toxin A or 300 ng/ml toxin B was added and the cells were incubated at 37°C for 3 h. The cells treated with GST-Srl (plus either toxin A or toxin B) were fixed with 3.7% paraformaldehyde followed by TRITC-phalloidin or Alexa 488-phalloidin, DAPI, and anti-Srl antibody labeling for observation by fluorescence microscopy or confocal laser microscopy (model no. LSM 710; Carl Zeiss). The percentage of cells adopting actin aggregate was determined by counting at least 300 cells from three randomly selected fluorescence microscopic fields in each of three independent wells (80 cells/field).

Cytotoxicity and antibody neutralization assays. MDCK and Caco-2 cells were used for the cytopathic effect (morphological change in cells) assays (37). The cells were seeded at 6×10^4 cells per well in 24-well plates and incubated for 48 h. Either toxin A (0.25 or 25 ng/ml) or toxin B (0.1 or 10 ng/ml) in the presence or absence of 10 μg/ml GST or GST-Srl was added to the cells, and they were incubated at 37°C for 24 h. The cells treated with toxin A or B (plus either GST-Srl or GST) were fixed with 3.7% paraformaldehyde followed by TRITC-phalloidin plus DAPI labeling for observation by fluorescence microscopy.

Cell viability based on cellular dehydrogenase activity was determined using both MDCK cells and human intestinal Caco-2 epithelial cells, as described elsewhere (19). The cells were seeded at 2.5×10^4 cells per well in 96-well plates. The plates were incubated for 48 h, and the culture medium was removed, after which cells were washed with serum-free medium. Specific concentrations of toxin A, toxin B, GST, GST-Srl alone, or GST/GST-Srl plus either toxin A or toxin B were added to the cells, and the cells were incubated at 37°C for 24 h. The value was determined with the metabolic indicator 3-(4,5-dimethylthiazol-2-yl)-5-(3-carboxymethoxyphenyl)-2-(4-sulfophenyl)-2H-tetrazolium salt (MTS) according to the manufacturer's instructions (Promega).

The release of oligonucleosomal DNA into the cytoplasm as a measure of apoptotic cell death was analyzed using the cell death detection enzyme-linked immunosorbent assay (ELISA) kit (Roche) according to the manufacturer's instructions. Briefly, MDCK or Caco-2 cells were seeded at 2.5×10^4 cells per well in 96-well plates. The plates were incubated for 48 h, and the culture medium was removed, after which cells were washed with serum-free medium. MDCK or Caco-2 cells were treated with indicated concentrations of toxin A, toxin B, GST, GST-Srl alone, or GST/GST-Srl plus either toxin A or toxin B for 24 h. The cells were then lysed, and the extracted cytoplasmic oligonucleosomal DNA was captured in ELISA wells containing anti-histone antibodies. The oligonucleosomal DNA was detected with an anti-DNA peroxidase-conjugated antibody. The absorbance of each well was determined using a microplate reader at 405 nm (Bio-Rad).

TER using polarized human intestinal Caco-2 cell monolayers was measured as described elsewhere (16). Briefly, Caco-2 cells were seeded at 5×10^4 cells per collagen-coated 24-transwell insert (BD Biosciences) and incubated for 1 week after reaching confluence (16 days in culture). Specific concentrations of toxin A, toxin B, GST, GST-Srl alone, or GST/GST-Srl plus either toxin A or toxin B were added to the apical or basolateral compartments, and the cells were incubated at 37°C until each time point. TER of the Caco-2 monolayers was measured using the Millicell Electrical Resistance System (Millipore) according to the manufacturer's instructions. The TER value was obtained by subtracting the resistance value of a transwell insert of cell-free culture medium.

For the antibody neutralization assays (26, 30, 33, 42) using affinity-purified anti-Srl antibody (200 μg/ml), MDCK or Caco-2 cells were seeded at 6×10^4 cells per well in 24-well plates and incubated for 24 h or 7 days, respectively. *C. difficile* culture filtrate was incubated with appropriately diluted anti-Srl antibody or control IgG (Cosmo Bio) for 1 h with gentle agitation before the serial dilutions. Serial dilutions of the neutralized culture filtrate were made in DMEM and added to the cells. The morphological changes were observed by fluorescence microscopy after 24 h of incubation followed by fixation and TRITC-phalloidin plus DAPI labeling. The cytopathic effect was determined as described previously (26, 37). The percentage of actin aggregate was determined as described above.

Statistical analysis. All values are expressed as means ± standard deviations (SD). For the statistical evaluation, Student's *t* test was performed, and *P* values of <0.05 were considered significant.

Nucleotide sequence accession number. The nucleotide sequences of *srl* of *C. difficile* strain ATCC 9689 were deposited in the DDBJ/EMBL/GenBank databases under accession number AB605620.

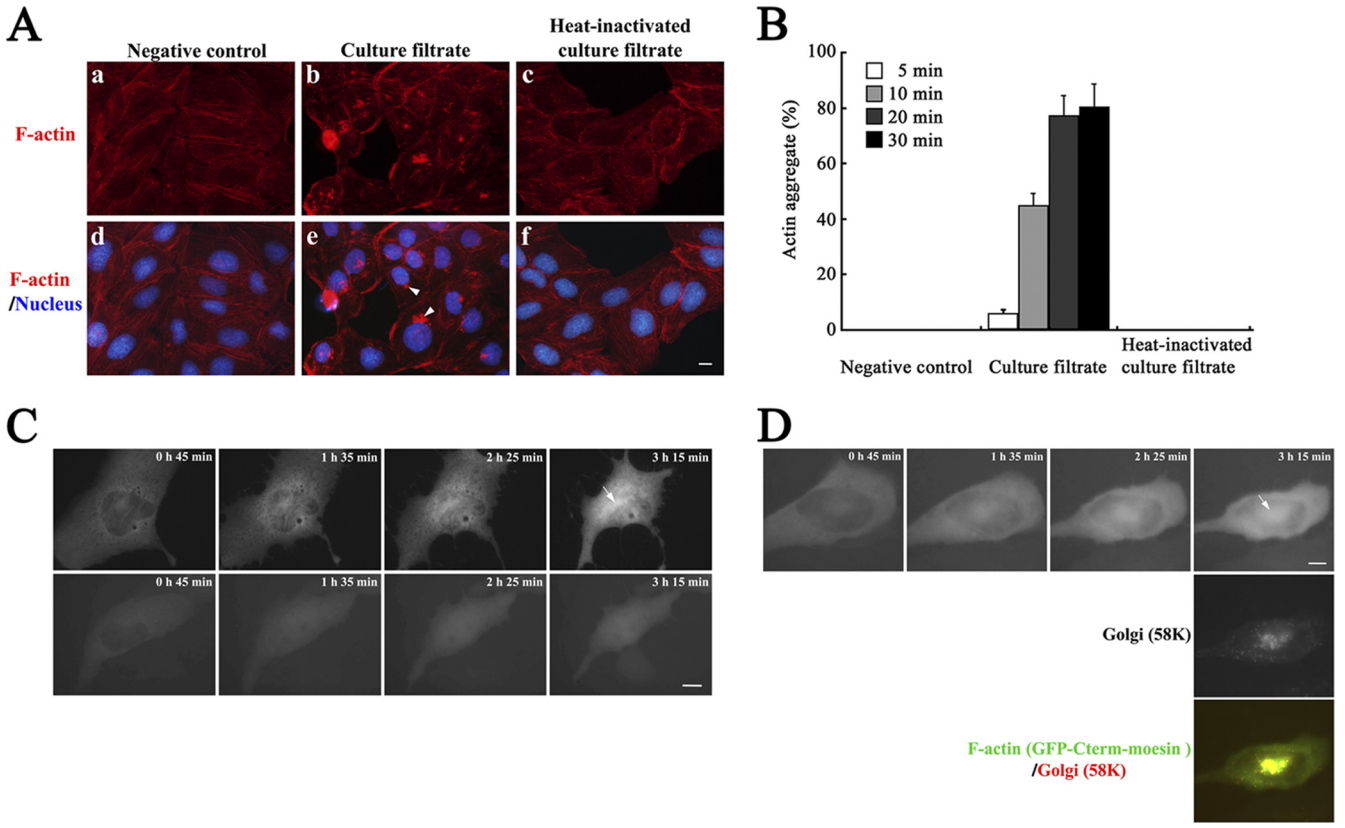

FIG. 1. Formation of actin aggregate at the juxtanuclear region in *C. difficile* culture filtrate-treated MDCK cells. (A) F-actin distribution in control cells (bacterium-free culture medium-exposed MDCK cells) (left panels), *C. difficile* culture filtrate-exposed MDCK cells (middle panels), and heat-inactivated *C. difficile* culture filtrate-exposed MDCK cells (right panels) after 30 min of culture filtrate exposure following medium replacement and 3 h of incubation. Images of TRITC-phalloidin-labeled F-actin (top panels) and merged images of DAPI-labeled nucleus with F-actin (bottom panels) are shown. The arrowheads in panel e indicate actin aggregate. Bar, 5 μm. (B) MDCK cells were treated with each preparation of culture filtrate in panel A for the indicated exposure times and further incubated for 3 h followed by labeling with TRITC-phalloidin and DAPI. The percentage of cells that formed actin aggregate was calculated. Results are means ± SD for three independent measurements. (C) Live-cell analysis of F-actin organization after *C. difficile* culture filtrate treatment (top panels) or 400 ng/ml toxin B treatment (bottom panels). Fluorescence images of GFP-Cterm-moesin-labeled F-actin are shown for each of the time points of observation. The arrow indicates actin aggregate. Bar, 5 μm. (D) After live-cell analysis of F-actin organization, cells were fixed and immunolabeled with anti-Golgi region 58K protein antibody and secondary Texas Red-conjugated antibody. Fluorescence images and the merged image (top, F-actin; middle, Golgi region; bottom, F-actin/Golgi region) are shown. The arrow indicates actin aggregate. Bar, 5 μm.

RESULTS

Golgi region-associated F-actin structure in *C. difficile* culture filtrate-treated cells. To describe cytopathic effects of *C. difficile* at early stages of intoxication, we monitored the F-actin cytoskeleton during the course of cell rounding by short-term treatment with a low-dilution *C. difficile* ATCC 9689 culture filtrate followed by replacement in fresh culture medium, which permits accessibility of minor proteins potentially produced by a *C. difficile* toxigenic strain to cells (9). After a 3-h treatment, TRITC-phalloidin staining demonstrated actinomorphic effects on MDCK cells, such as the disappearance of the actin cytoskeleton and a distorted cortical actin structure. These affected cells are well defined as a prerequisite for characteristic cell rounding caused by toxins (1, 9, 10). Notably, aggregation of F-actin at the polar juxtanuclear position was observed (Fig. 1A, panels b and e). We termed this F-actin aggregated structure "actin aggregate," as this structure has not been previously characterized in toxin-exposed epithelial cells. To test whether proteinaceous factors were involved in the formation of the actin aggregate, proteins in the culture filtrate were heat inactivated (incubated at 95°C for 5 min). On the contrary, MDCK cells treated with a heat-inactivated *C. difficile* culture filtrate did not show any cytopathic effects, including actin aggregate (Fig. 1A, panels c and f). The frequency of visible actin aggregate was markedly increased in a time-dependent manner after culture filtrate exposure (Fig. 1B). To exclude conditions that may affect actin integrity such as fixation or shifts in temperature, images were acquired on live cells at 37°C by monitoring F-actin dynamics in live cells (8). MDCK cells were transfected with a plasmid encoding the GFP-fused C-terminal actin-binding domain of moesin and treated with *C. difficile* culture filtrate. Within 3 h after treatment, actin aggregate was visible at the juxtanuclear position (upper panels in Fig. 1C). Treatment with purified toxin A or B did not trigger actin aggregate, although cell shrinkage was observed (bottom panels in Fig. 1C [data are shown only for toxin B]). The juxtanuclear position of actin aggregate was comparable to that of the Golgi complex. In fact, immunola-

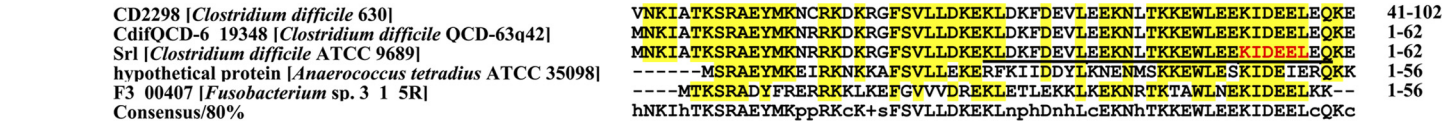

FIG. 2. Alignment of Srl homologs. Homologs were identified by PSI-BLAST searches of the NCBI database using the CD2298 amino acid sequence from *C. difficile* CD630 as the query sequence. An E value of $<1e-5$ was chosen as a cutoff value for significance. Srl cognate proteins are present in other opportunistic pathogenic bacteria, including *Anaerococcus* and *Fusobacterium* species. The KIDEEL sequence in Srl is noted by red letters. A synthetic peptide sequence used for antibody production is underlined. Alignment is presented using CHROMA to yellow columns with 80% conservation. Consensus abbreviations (shown below alignment): h, hydrophobic (ACFGHILMTVWY); p, polar (CDEHKNQRST); s, small (ACDGNPSTV); c, charged (DEHKR); n, negatively charged (DE); +, positively charged (HKR).

beling for the Golgi marker 58K protein showed significant colocalization of actin aggregate at the position of the Golgi region (Fig. 1D). These results suggest that a proteinaceous factor(s) other than toxins A and B in *C. difficile* culture filtrate is involved in the formation of juxtanuclear actin aggregate in MDCK cells.

Srl bearing a KDEL-like sequence is present in the culture filtrate of *C. difficile* strain ATCC 9689. Some known bacterial toxins such as heat-labile toxin of toxigenic *E. coli* and cholera toxin, which employ the Golgi region-associated retrograde transport pathway, have a characteristic KDEL (Lys-Asp-Glu-Leu) or KDEL-like motif at their C termini. This motif recognizes the KDEL receptor in host cells for retro-transport of these toxins from the Golgi region to the endoplasmic reticulum, an important role for the cytotoxicity of these toxins (6, 25, 27). Although the KDEL motif has not been reported in known *C. difficile* toxins, we hypothesized that a factor which has a KDEL(-like) motif produced in *C. difficile* culture filtrate reaches the Golgi region, where it affects the organization of the F-actin cytoskeleton in cells.

To find a candidate responsible for the observed actin aggregate, we searched the genome sequence of *C. difficile* strain CD630, which has been well characterized for protein coding sequences (38). Because the KDEL motif is known to be located at the C-terminal end of the protein, we focused on the C-terminal 10-amino-acid sequences in 931 hypothetical proteins as candidates in the *C. difficile* strain CD630 genome (NCBI accession no. NC009089). One candidate annotated as the hypothetical protein "CD2298" was chosen. It bears the KDEL-like "KIDEEL" sequence near the C terminus; although a landmark for the search was the KDEL motif itself, variations of the motif in the number and sequence of amino acids have been reported (25, 43). The protein sequence of CD2298 was subjected to BLAST analysis and used for alignment (Fig. 2). Putative homologs or truncated versions of CD2298 were also found to be conserved in *C. difficile* toxigenic strain QCD-63q42 and opportunistic pathogens *Anaerococcus tetradius* and *Fusobacterium* species (Fig. 2).

The presence of the candidate gene in *C. difficile* strain ATCC 9689 was examined by PCR using primers flanking the coding sequences of CD2298. We observed an amplicon of the expected size for the candidate gene, which we used as a template for DNA sequencing. The resulting DNA sequence encoded a protein (GENETYX software) which was identical to the hypothetical protein "QCD19345" in *C. difficile* toxigenic strain QCD-63q42 (Fig. 2). It retained the C-terminal KIDEEL sequence but no signal peptide or known domain structures (BLAST analysis). We named this protein coding sequence *srl* for sensitivity regulation. Polyclonal antibodies were raised against a synthetic peptide corresponding to the C-terminal portions of Srl (underlined in Fig. 2) and used to detect protein products of *srl* on Western blots. A single protein band of the expected size (7.6 kDa) was detected in samples from both TCA-precipitated culture filtrate and whole-cell lysate of *C. difficile* strain ATCC 9689 but not in samples from an irrelevant clostridial strain, *C. novyi* ATCC 17861 (Fig. 3A), suggesting the production and secretion of Srl from *C. difficile* strain ATCC 9689. To determine whether Srl is conserved among *C. difficile* strains, we performed a Western blot analysis to survey 26 clinical isolates (Fig. 3B). In total, 21 of 26 strains produced Srl. Both toxigenic type A^+ B^+ *C. difficile* strains (19/21) and toxigenic type A^- B^- strains (2/5) produced Srl, suggesting that the prevalence of Srl-producing *C. difficile* strains is not low.

Srl together with either toxin A or toxin B is responsible for the formation of F-actin-aggregated structures in cells. To investigate whether Srl is involved in the observed actin aggregation in cells, Srl protein was fused to GST at the N terminus and purified from an *E. coli* cell line containing a recombinant GST-Srl gene in its plasmid (Fig. 4A). MDCK cells were treated for 3 h with GST-Srl or GST as a control. No morphological changes in the cells or alterations in the organization of F-actin were observed (Fig. 4B, panel b). Similar results were obtained with a treatment of 10 μg/ml GST-Srl for 24 h (data not shown), suggesting that the GST-tagged Srl itself could not affect the organization of F-actin in cells. We speculated that some additional factors may be required for triggering actin aggregation. There are no domain structures within the entire amino acid sequence of Srl known to be involved in the modulation of the actin cytoskeleton (BLAST analysis); therefore, both Srl and *C. difficile* toxin(s) are thought to be required for the formation of the actin aggregate. To test this hypothesis, we used both purified toxin A and toxin B in the following experiment because both toxins are reported to be key virulence factors of *C. difficile* (26, 30). The binary toxin (CDT) was excluded as a candidate because *cdtA* was not conserved in the *C. difficile* ATCC 9689 genome as analyzed by Southern blotting (data not shown). When cells were treated with purified GST-Srl plus either toxin A or toxin B for 3 h, a structure of actin aggregate was observed at one polar juxtanuclear position in the cells (Fig. 4B, panels d and f, and arrowheads in panels j and l), suggesting that both GST-Srl and either toxin A or toxin B are sufficient in triggering the formation of an actin aggregate in the cells.

A KDEL-like sequence in Srl prompted us to examine the localization of GST-Srl in cells. MDCK cells treated with GST-

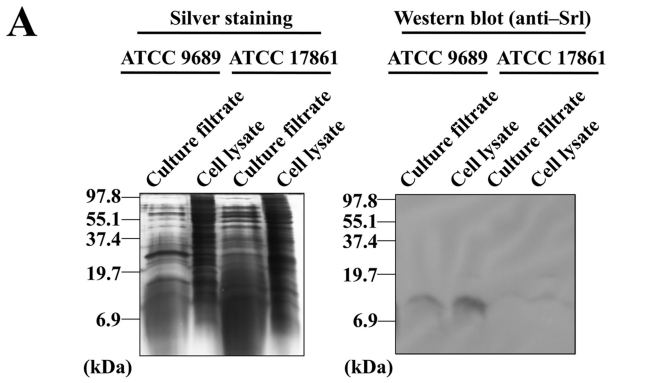

Strain #	Toxin A	Toxin B	Srl	Strain #	Toxin A	Toxin B	Srl
1	+	+	+	14	-	-	+
2	+	+	+	15	+	+	+
3	+	+	+	16	-	-	-
4	+	+	+	17	+	+	+
5	+	+	+	18	+	+	+
6	+	+	+	19	-	-	+
7	+	+	+	20	+	+	+
8	+	+	+	21	+	+	+
9	+	+	-	22	+	+	+
10	+	+	+	23	-	-	-
11	+	+	+	24	+	+	-
12	+	+	+	25	+	+	+
13	-	-	-	26	+	+	+

FIG. 3. Production of Srl in *C. difficile* ATCC 9689 and clinical strains. (A) Whole-cell lysate and TCA-precipitated culture filtrate from *C. difficile* ATCC 9689 or *C. novyi* ATCC 17861 as the negative control were subjected to SDS-PAGE followed by silver staining. The same samples were analyzed by Western blotting with polyclonal anti-Srl antibody. (B) Whole-cell lysate of each strain was subjected to Western blotting with polyclonal anti-Srl antibody. For detection of toxins A and B, membrane-based enzyme immunoassays were performed. The results are summarized in the table; + and − denote positive and negative results, respectively, of enzyme immunoassay for toxins A and B or Western blotting for Srl.

Srl alone or GST-Srl in the presence of either toxin A or toxin B for 3 h were subjected to immunofluorescent microscopy using an anti-Srl antibody. Cells treated with GST-Srl and either toxin A or toxin B exhibited one polar juxtanuclear staining of GST-Srl (Fig. 4B, panels p and r), but none were seen in cells treated with GST-Srl alone. The observed localization of GST-Srl at the juxtanuclear position was consistent with the localization of the actin aggregate structure. In fact, the juxtanuclear accumulations of GST-Srl and the actin aggregate were significantly colocalized in the cells (Fig. 4B, arrowheads in panels v and x). A similar subcellular colocalization of GST-Srl and actin aggregate was observed by confocal microscopy (Fig. 4C [data are shown only for toxin B]). These observations are consistent with the hypothesis that Srl together with either toxin A or toxin B is responsible for the formation of an actin aggregate in cells.

To further examine the involvement of GST-Srl in the formation of the cellular actin aggregate, MDCK cells were treated with toxin A, toxin B, GST, GST-Srl alone, or GST/GST-Srl plus either toxin A or toxin B, and the percentage of cells that formed an actin aggregate was calculated (Fig. 4D). GST-Srl alone and GST alone did not cause any actin aggregation in cells. As expected, GST-Srl increased the frequency of actin aggregate-positive cells in the presence of either toxin A or toxin B (more than 79%), whereas GST in the presence of toxin A or B did not. However, treatment with either toxin A or toxin B alone induced actin aggregation in a small number of cells (less than 4%). When MDCK cells were treated with serial concentrations of GST-Srl or GST in the presence of either toxin A or toxin B (Fig. 4E), the frequency of actin aggregate-positive cells clearly increased in a GST-Srl concentration-dependent manner. These results suggest that both toxin A and toxin B can induce the formation of F-actin-aggregated structures, the frequency of which can be enhanced by the presence of GST-Srl.

To test whether simultaneous presence of GST-Srl with either toxin A or B is required to increase the frequency of actin aggregate-positive cells as well as the subcellular localization of GST-Srl, MDCK cells were pretreated with GST-Srl for 3 h and then GST-Srl was washed off before addition of either toxin A or B (Fig. 4D). Removal of GST-Srl from MDCK cells dramatically reduced the frequency of actin aggregate-positive cells to levels similar to treatment with each toxin alone. In addition, immunofluorescent microscopy using anti-Srl antibody did not exhibit any juxtanuclear staining of GST-Srl in cells (data not shown), suggesting that GST-Srl alone does not have any effect on the toxin-induced actin arrangement.

Srl enhances cytotoxicity of *C. difficile* toxins A and B. We reasoned that if the formation of actin aggregates was triggered by toxins and enhanced by the presence of Srl, mixtures of Srl and either toxin A or B might induce increased morphological changes of the cells into rounded shapes as described by the cytopathic effect. To test this possibility, MDCK cells were treated for 24 h with GST-Srl or GST in the presence of either toxin A or toxin B (Fig. 5A). While treatment of GST with 0.25 ng/ml toxin A had no morphological effect on the MDCK cells due to the low dosage of the toxin (Fig. 5A, panel c), treatment of GST-Srl with 0.25 ng/ml toxin A was sufficient in causing morphological changes in the cells (Fig. 5A, panel d). Similarly, while treatment of GST with 25 ng/ml toxin A was sufficient in causing morphological changes in the cells (Fig. 5A, panel j), treatment of GST-Srl with 25 ng/ml toxin A caused complete rounding of almost all the cells (Fig. 5A, panel k). Similar GST-Srl-enhanced cytopathic effect was observed in the cells with 0.1 ng/ml toxin B (Fig. 5A, panel g) or 10 ng/ml toxin B (Fig. 5A, panel n). These results suggest that Srl enhances toxin-mediated disorganization of the F-actin structure in epithelial cells.

The recombinant Srl-enhanced toxin-mediated cell rounding prompted us to measure changes in the viability of Srl- and toxin-treated cells. Changes in cell viability were assessed using an aqueous soluble tetrazolium/formazan assay. While 250 ng/ml toxin A alone induced an approximate 40% drop in viability after a 24-h treatment in MDCK cells, the viability of 100 ng/ml toxin B-treated cells induced an approximate 30% drop. In contrast, 10 μg/ml GST-Srl alone did not cause any changes in cell viability (Fig. 5B), suggesting that GST-Srl itself does not influence the viability of the cells. To test whether Srl affects either toxin A- or B-induced decreases in cell viability,

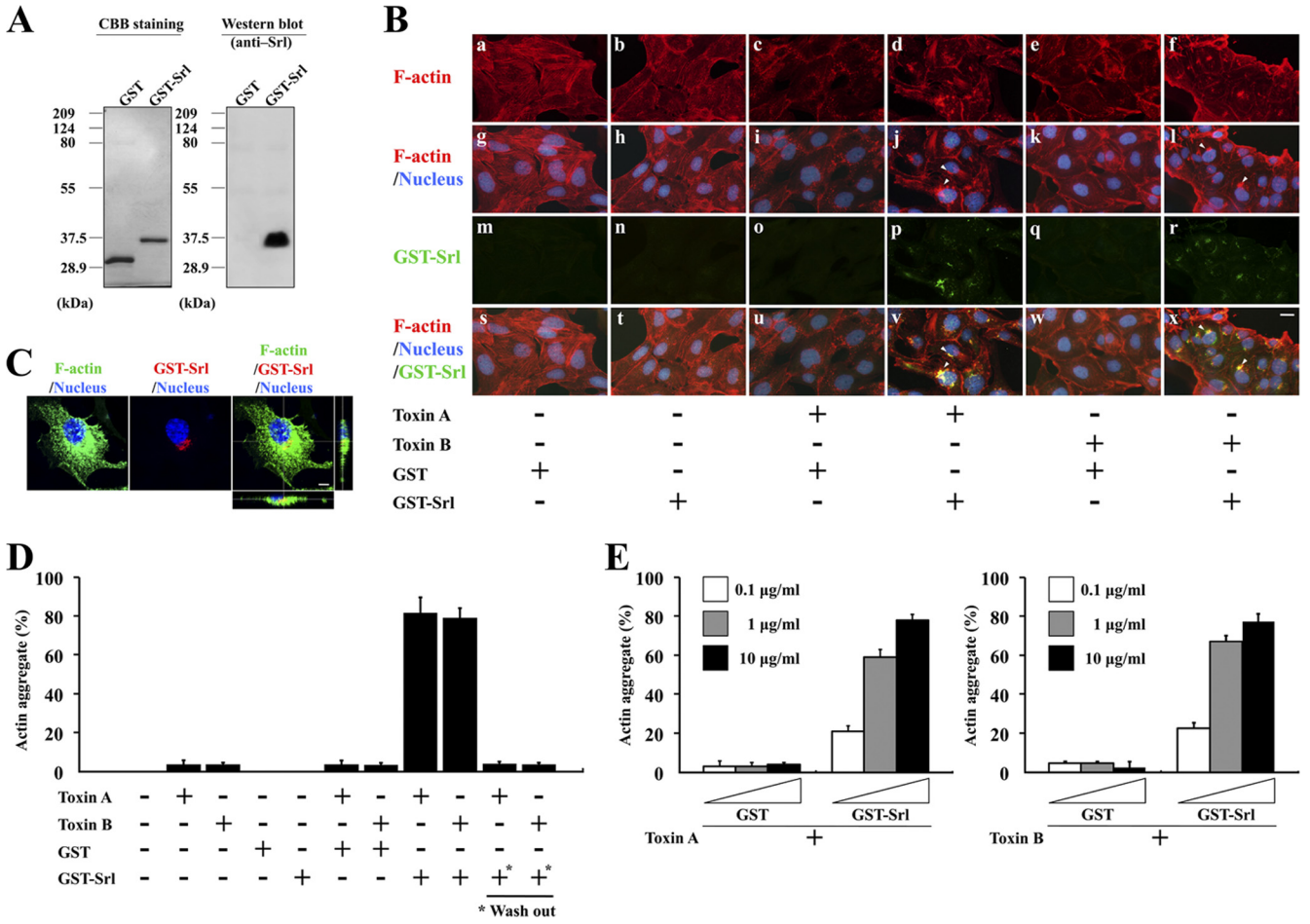

FIG. 4. Treatment with GST-Srl and either toxin A or toxin B triggers increased formation of an actin aggregate in cells. (A) Purified GST-Srl was subjected to SDS-PAGE and CBB staining or Western blotting. For CBB staining, 0.2 μg purified protein was loaded on the gel. For Western blotting, a 1:10 dilution of the samples was used. (B) MDCK cells were treated for 3 h with 10 μg/ml GST-Srl or GST in the absence or presence of 750 ng/ml toxin A or 300 ng/ml toxin B and then subjected to immunofluorescent microscopy using anti-Srl antibody. F-actin and DNA were stained with TRITC-phalloidin and DAPI, respectively. Fluorescence images and the merged images are shown. Bar, 10 μm. Arrowheads in panels j and l indicate actin aggregates. Arrowheads in panels v and x indicate the sites of accumulation of GST-Srl. (C) Subcellular localization of GST-Srl. MDCK cells treated with 10 μg/ml GST-Srl plus 300 ng/ml toxin B for 3 h were stained with Alexa 488-phalloidin (green), an anti-Srl antibody (red), and DAPI (blue). Bar, 5 μm. (D) MDCK cells were treated for 3 h with 750 ng/ml toxin A, 300 ng/ml toxin B, 10 μg/ml GST-Srl, 10 μg/ml GST alone, or indicated combinations of GST-Srl or GST and either toxin, and the percentage of cells that formed an actin aggregate was calculated. Results are means ± SD of three independent measurements. + and − denote positive and negative results, respectively. *, MDCK cells that were pretreated for 3 h with 10 μg/ml GST-Srl, after which GST-Srl was washed off before either toxin A or B was added. (E) MDCK cells were treated for 3 h with the indicated concentrations of GST-Srl or GST in the presence of either 750 ng/ml toxin A or 300 ng/ml toxin B, and the percentage of cells that formed an actin aggregate was calculated. Results are means ± SD of three independent measurements.

MDCK cells were treated with serial concentrations of GST-Srl or GST in the presence of either toxin A or toxin B and the cell viabilities were measured (Fig. 5C). While treatment of 10 μg/ml GST with toxin A had no effect on the decrease in the cell viability of MDCK cells (an approximate 40% decrease that is consistent with treatment of toxin A alone), a 24-h treatment of 10 μg/ml GST-Srl with toxin A resulted in an approximate 60% decrease of cell viability (Fig. 5C, left side). Similar results were obtained when treatments of 10 μg/ml GST plus toxin B and 10 μg/ml GST-Srl plus toxin B (decreases of 29% and 45%, respectively; Fig. 5C, right side) were compared. In the presence of GST-Srl plus either toxin A or toxin B, the enhanced reduction in cell viability was observed in a GST-Srl concentration-dependent manner.

One may speculate that the enhanced decrease in cell viability after treatment with Srl plus either toxin A or toxin B may be involved in the increased apoptosis, since both toxin A and toxin B are reported to induce apoptotic cell death (5, 17, 31). Thus, the effect of Srl on toxin-mediated cell death was assessed by measuring apoptotic oligonucleosomal DNA fragmentation (Fig. 5D and E). While toxin A or toxin B alone induced apoptotic DNA fragmentation in MDCK cells at 24 h, GST-Srl alone did not cause any increase in DNA fragmentation in the cells (Fig. 5D). In contrast, GST-Srl plus either toxin A or toxin B showed increased apoptotic DNA fragmentation of cells at 24 h in a GST-Srl concentration-dependent manner compared to that of cells treated with GST with either toxin (Fig. 5E). Taken together, these results suggest that Srl

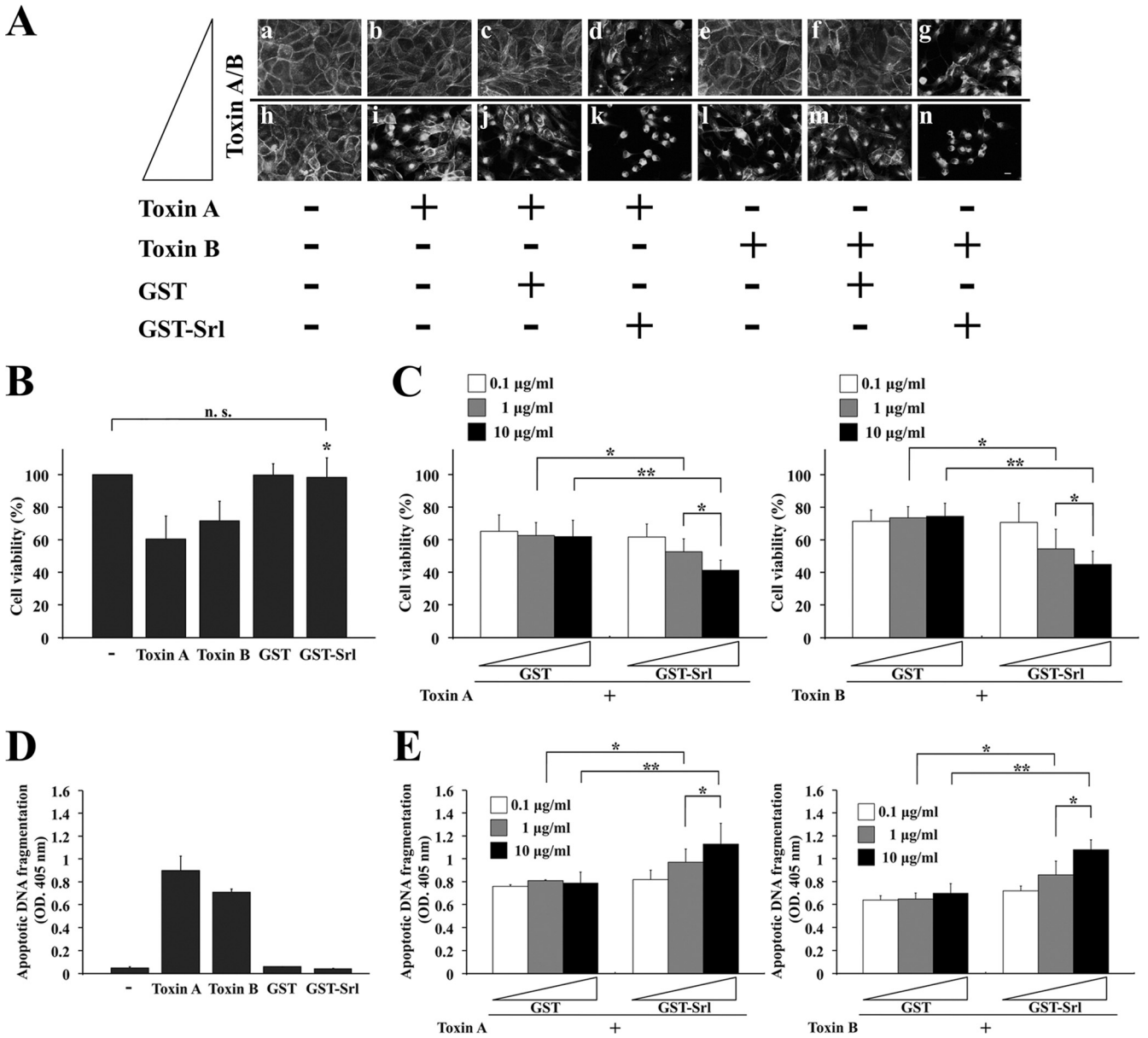

FIG. 5. GST-Srl enhances the cytotoxicity of both toxin A and toxin B in epithelial cells. (A) Morphological changes of MDCK cells after treatment with toxin A (0.25 ng/ml [panels b, c, and d] versus 25 ng/ml [panels i, j, and k]) or toxin B (0.1 ng/ml [panels e, f, and g] versus 10 ng/ml [panels l, m, and n]) in the presence of either GST-Srl or GST. After 24 h of incubation, cells were fixed and labeled with TRITC-phalloidin. + and − denote positive and negative results, respectively. Bar, 10 μm. (B) MDCK cells were incubated with 250 ng/ml toxin A, 100 ng/ml toxin B, 10 μg/ml GST-Srl, or 10 μg/ml GST alone. After incubation for 24 h, cell viability was measured by an aqueous soluble tetrazolium/formazan assay and expressed as a percentage of the results from buffer-treated controls (−). All reactions were performed in triplicate, and the results are means ± SD of three independent measurements. n.s., not significant. *, $P < 0.01$ versus toxin A or toxin B. (C) MDCK cells were incubated for 24 h with the indicated concentrations of GST-Srl or GST in the presence of either 250 ng/ml toxin A or 100 ng/ml toxin B. The viability of MDCK cells was determined as in panel B. Results are means ± SD of three independent measurements. *, $P < 0.05$; **, $P < 0.01$. (D) MDCK cells were incubated with 250 ng/ml toxin A, 100 ng/ml toxin B, 10 μg/ml GST-Srl, or 10 μg/ml GST alone. After incubation for 24 h, lysates were prepared, and apoptotic oligosomal DNA fragmentation was assessed using a cell death ELISA kit. All reactions were performed in triplicate, and the results are expressed as optical density (OD.) at 405 nm. Mean values ± SD are indicated for three independent measurements. −, buffer-treated control. (E) MDCK cells were incubated for 24 h with the indicated concentrations of GST-Srl or GST in the presence of 250 ng/ml toxin A or 100 ng/ml toxin B. The cell death induced in MDCK cells was detected as in panel D. *, $P < 0.05$; **, $P < 0.01$.

enhances the cytotoxicity of both toxin A and toxin B, although it does not have any observable cytotoxic activity of its own.

To exclude cell line-specific effects, we tested Caco-2 cells in a comparable assay. Similar to the results for MDCK cells, in which actin-aggregated structures were sometimes observed after treatment with toxin A or toxin B alone and not in cells treated only with GST-Srl (data not shown), actin-aggregated structures were frequently observed in Caco-2 cells treated

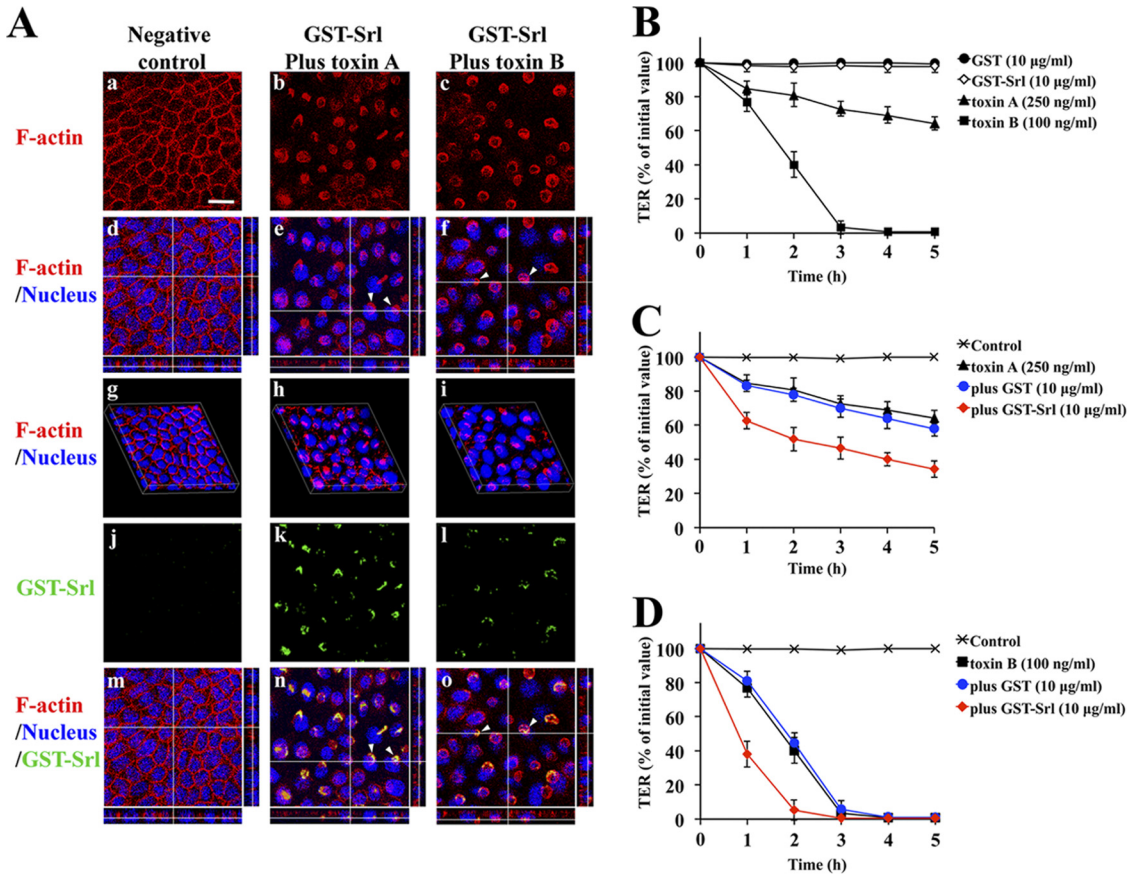

FIG. 6. Enhancement of actin rearrangement and toxin-mediated cytotoxicity by recombinant Srl (GST-Srl) in human colon carcinoma cells. (A) A Caco-2 cell monolayer grown on a glass coverslip was incubated for 3 h with 10 μg/ml GST-Srl in the presence of either 750 ng/ml toxin A or 300 ng/ml toxin B. Cells were fixed, stained with phalloidin (red), anti-Srl antibody (green), and DAPI (blue), and then visualized by confocal microscopy. Confocal images of F-actin only (panels a, b, and c) and x–y, x–z, and y–z sectional views of the merged images are shown (panels d, e, and f, respectively). Confocal images of GST-Srl only (panels j, k, and l) and x–y, x–z, and y–z sectional views of the merged images are shown (panels m, n, and o, respectively). Reconstructed 3D images are also shown (panels g, h, and i). Negative control denotes buffer-treated cells. Bar, 20 μm. Arrowheads in panels e and f point to the actin aggregate at the apical side of the cells. Arrowheads in panels n and o point to the sites of accumulation of GST-Srl. (B) TER was measured at hourly time intervals after apical treatment of Caco-2 monolayers with toxin A, toxin B, GST, or GST-Srl. Results are means ± SD of four independent measurements. (C) Caco-2 monolayers were incubated with 10 μg/ml GST-Srl or GST in the presence of 250 ng/ml toxin A in the apical compartment. Results are means ± SD of four independent measurements. Control denotes buffer-treated cells. (D) Results of an experiment similar to that in panel C but in the presence of 100 ng/ml toxin B. Results are means ± SD of four independent measurements.

with GST-Srl with either toxin A or toxin B (Fig. 6A, panels b and c). Confocal analysis of z-stack images showed that the actin rearrangement occurred mainly near the apical surface of the Caco-2 cells (Fig. 6A, arrowheads in panels e and f). The three-dimensional (3D) images demonstrated that the F-actin architecture of the monolayer, which delineates the cell peripheries, was also perturbed by the treatment of GST-Srl plus either toxin A or B (Fig. 6A, panels h and i), emphasizing that the disturbance of cytoskeletal architecture induced by either toxin is enhanced by Srl. It is noteworthy that in immunofluorescent analysis cells treated with GST-Srl plus either toxin A or toxin B exhibited juxtanuclear staining of GST-Srl (Fig. 6A, panels k and l). The observed localization of GST-Srl at the juxtanuclear position was associated with that of the actin aggregate structure (Fig. 6A, arrowheads in panels n and o). These results are in good agreement with immunofluorescence data shown in Fig. 4B.

Srl enhances both toxin A- and B-induced decreases in TER of human intestinal cells. Measurement of TER decreases is known to be useful in characterizing both toxin A- and B-mediated cytopathic effects (35). To examine whether Srl has cytotoxicity in intestinal epithelial cells, TER was measured for 5 h at hourly time intervals after apical treatment of Caco-2 monolayers with toxin A, toxin B, GST, or GST-Srl alone. While a treatment of 100 ng/ml toxin B induced a profound drop in TER within 3 h, treatment of 250 ng/ml toxin A induced a more delayed drop in TER due to the low susceptibility of Caco-2 cells to toxin A. In contrast, 10 μg/ml GST-Srl did not affect TER, suggesting that the recombinant Srl itself does not influence intestinal barrier function (Fig. 6B). We reasoned that if the cytoskeletal disorganization was triggered by either toxin A or B and enhanced by the presence of Srl, the simultaneous presence of GST-Srl and either toxin A or toxin B might affect the barrier functions of epithelial cells more

than toxin treatment alone. To test this hypothesis, Caco-2 monolayers were treated in the apical compartment with 10 μg/ml GST-Srl or GST in the presence of either toxin A or toxin B and TER was monitored (Fig. 6C and D). While treatment of GST plus toxin A had no additional effect on the TER decrease, treatment of GST-Srl plus toxin A showed an enhanced drop in TER at early time points. Similar results were obtained with toxin B (Fig. 6D). Time course experiments for the enhanced drop in TER were similar irrespective of apical or basolateral application of the same samples (data not shown). Enhanced increases in both toxin-mediated cell rounding and DNA fragmentation and decrease in cell viability from the addition of GST-Srl plus either toxin A or B were also observed in Caco-2 cells (data not shown), indicating that Srl enhances the cytotoxicity of both toxin A and toxin B in human intestinal epithelial cells.

Srl in culture filtrate is involved in both the formation of actin aggregates and the enhanced cytopathic effect. We reasoned that if Srl enhances both toxin A- and toxin B-mediated cytotoxicity, actin aggregation might be a feature of the enhanced cytotoxicity. To test this hypothesis, we examined whether antibody-mediated neutralization of Srl in culture filtrate results in the partial neutralization of cytotoxicity of both toxins A and B and the disappearance of actin aggregate. *C. difficile* ATCC 9689 culture filtrate was incubated with anti-Srl antibody or control IgG for 1 h and then used to treat MDCK cells for 24 h. The culture filtrate with anti-Srl antibody showed decreased cytopathic effects (morphological changes) in an anti-Srl-antibody concentration-dependent manner compared to those with control IgG (Fig. 7A). Furthermore, phalloidin staining of MDCK cells treated for 3 h with the Srl-neutralized culture filtrate demonstrated significantly fewer actin aggregates in cells in an anti-Srl-antibody concentration-dependent manner than in control IgG (Fig. 7B). Similar results were obtained for the decreased cytopathic effect and formation of actin aggregates by the treatment with Srl-neutralized culture filtrate to Caco-2 cells (data not shown). These results suggest that Srl in the culture filtrate is involved in both the increased cytotoxicity of toxins A and B and the formation of the actin aggregate in cells.

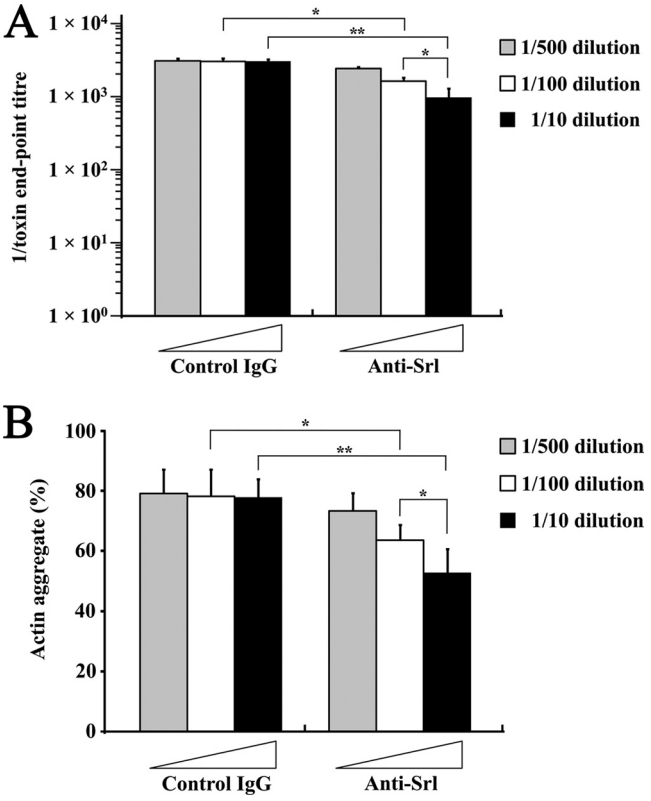

FIG. 7. Partial inhibition of morphological changes with Srl-neutralized culture filtrate in parallel with decreased formation of the actin aggregate in cells. (A) *C. difficile* ATCC 9689 culture filtrate was prepared by incubation with anti-Srl antibody or control rabbit IgG for 1 h at the indicated concentrations. MDCK cells were then treated for 24 h with a preparation of the culture filtrate, and morphological changes (the cytopathic effect) of the cells were scored by dilution endpoints. Results are means ± SD of three independent measurements. *, $P < 0.01$; **, $P < 0.001$. (B) MDCK cells were treated for 3 h with a preparation of *C. difficile* ATCC 9689 culture filtrate. Cells were fixed and stained with TRITC-phalloidin and DAPI. The percentage of cells that formed an actin aggregate was calculated. Results are means ± SD of three independent measurements. *, $P < 0.05$; **, $P < 0.01$.

DISCUSSION

In this study, we characterized Srl in *C. difficile* ATCC 9689 and demonstrated that Srl plays a role in enhancing the cytotoxicity of both toxin A and toxin B but that the Srl-fusion protein alone has no detectable cytotoxic activity. However, our findings do not exclude the possibility that Srl is a minor toxin with activity that might potentially be inhibited within the fusion protein.

Under the presence of GST-Srl plus either toxin A or toxin B or by treatment with culture filtrate, we observed a previously uncharacterized actin-aggregated structure at the juxtanuclear region of MDCK cells. Meyer et al. previously reported that toxin B caused juxtanuclear condensation of F-actin in cultured mast cells (32), suggesting that toxin B itself has potency in inducing F-actin structures at juxtanuclear positions of cells. Possibly the combination of both the treatment with a high concentration of either toxin A or toxin B and the high sensitivity of those cells to the toxins might result in the formation of F-actin aggregate in the juxtanuclear region due to an intensified effectiveness of glucosyltransferase activity of the toxins for inactivation of Rho GTPases. Since tagged Srl alone showed no detectable cytotoxicity and did not contain any domain structures predicted to be involved in F-actin modulation, and because actin aggregates were observed infrequently (less than 4%) in MDCK cells treated with either purified toxin A or toxin B alone (Fig. 4D), the role of Srl may be in sensitizing cells to the two glucosylating toxins. Juxtanuclear disorganization of F-actin in cells could be triggered by toxin A or toxin B alone based on the fact that the regulation of protein transport between the ER and the Golgi region as well as actin polymerization is mainly controlled by RhoA, RhoB, RhoG, and Cdc42 (11, 20, 28), which are targets of glucosylation by both toxins. Similar formation of actin aggregates in cells treated with a combination of GST-Srl and either toxin A or toxin B (Fig. 4B and D and Fig. 6A) further supports the notion that the common toxic function of toxin A and toxin B is enhanced by Srl.

Our *in vitro* cytotoxicity assays demonstrated enhanced cytotoxicity of both toxin A and toxin B in the presence of tagged Srl (Fig. 5). These results are consistent with the putative role of Srl in sensitizing cells to both toxins. We reasoned that if the actin aggregate in cells sensitized by Srl was induced by the toxins, this actin aggregation phenotype should be paralleled by enhanced cytotoxic effects. In fact, when Srl was neutralized in culture filtrates, the observed partial neutralization of cytopathic morphological changes was consistent with a decrease in the formation of actin aggregates in cells (Fig. 7). Along this line, the formation of juxtanuclear F-actin-aggregated structures in cells might be a characteristic of the enhanced activity of both toxin A and toxin B by the "toxin sensitizer," Srl. The molecular mechanisms underlying these processes remain unknown. Recently, a reverse genetics system has been established and utilized for *C. difficile* (15, 24, 26, 30), and its application to Srl will be needed in future studies in order to definitively determine the role and the molecular mechanisms of Srl in the pathogenesis of *C. difficile* infection.

Srl was detected in both culture filtrates and whole-cell lysates of *C. difficile* ATCC 9689 (Fig. 3A). The protein, which is common among clinical isolates of *C. difficile* (Fig. 3B), may have access to intestinal epithelial cells after colonization of *C. difficile*. Since Srl comprises no detectable signal peptide, an unknown secretion mechanism may be involved. The observed subcellular localization of tagged Srl in the presence of either toxin A or toxin B (Fig. 4B and C and Fig. 6A) suggests that Srl can internalize into toxin-exposed epithelial cells. After removal of GST-Srl from GST-Srl-pretreated cells, neither toxin A nor B showed any enhanced induction of actin aggregates in juxtanuclear staining of Srl (data not shown; Fig. 4D), emphasizing that the simultaneous presence of both GST-Srl and either toxin is required for enhanced actin rearrangement as well as Srl internalization. These results support the notion that Srl internalization could be triggered in a toxin A-, toxin B-, or both toxin A- and B-induced cytopathic effect-dependent pathway (9, 10). In this process, the KDEL-like sequence KIDEEL in Srl may be involved. Thus, the putative role of Srl in cytotoxic activity appears to be as a "toxin sensitizer" based on the fact that the site of GST-Srl accumulation in cells was colocalized significantly with either toxin A- or toxin B-induced actin-aggregated structures that might be a feature of sensitized cells (Fig. 4B and 6A).

In summary, this study demonstrated for the first time a potential virulence role of Srl in the modulation of toxin sensitivity of epithelial cells by enhancing the cytotoxicity of both toxin A and B and concomitantly forming a F-actin structure localized at the juxtanucleus. Studies on the cytotoxic action of the *C. difficile* toxins have established the basis for its pathogenicity. Thus, an understanding of the toxin activity-modulating mechanism of Srl may improve the prospect of preventing and treating the pathological development of *C. difficile*.

ACKNOWLEDGMENTS

We are very grateful to A. Oga and K. Negayama for their assistance in bacterial culturing, H. Tazawa and K. Bou for their critical support, and Y. Aizawa, I. Okayasu, and T. Akahoshi for their helpful discussions. We thank T. Sasahara for providing MDCK cell lines, M. Ohnishi and H. Watanabe for the HeLa cDNA library and pGFP-moesin actin binding domain fusion construct, and T. Shimizu and S. Miyata for *E. coli* strains and purified clostridial toxins.

This work was implemented as a SRL, Inc., endowed course in Kitasato University School of Medicine and was supported by a grant from the Ministry of Education, Science and Technology of Japan.

REFERENCES

1. **Ahlgren, T., I. Florin, C. Jarstrand, and M. Thelestam.** 1983. Loss of surface fibronectin from human lung fibroblasts exposed to cytotoxin from *Clostridium difficile*. Infect. Immun. **39:**1470–1472.
2. **Aktories, K.** 1997. Bacterial toxins that target Rho proteins. J. Clin. Invest. **99:**827–829.
3. **Bartlett, J. G.** 2006. Narrative review: the new epidemic of *Clostridium difficile*-associated enteric disease. Ann. Intern. Med. **145:**758–764.
4. **Bélanger, S. D., M. Boissinot, N. Clairoux, F. J. Picard, and M. G. Bergeron.** 2003. Rapid detection of *Clostridium difficile* in feces by real-time PCR. J. Clin. Microbiol. **41:**730–734.
5. **Brito, G. A., et al.** 2002. Mechanism of *Clostridium difficile* toxin A-induced apoptosis in T84 cells. J. Infect. Dis. **186:**1438–1447.
6. **Cieplak, W., Jr., R. J. Messer, M. E. Konkel, and C. C. Grant.** 1995. Role of a potential endoplasmic reticulum retention sequence (RDEL) and the Golgi complex in the cytotonic activity of *Escherichia coli* heat-labile enterotoxin. Mol. Microbiol. **16:**789–800.
7. **Ciesla, W. P., Jr., and D. A. Bobak.** 1998. *Clostridium difficile* toxins A and B are cation-dependent UDP-glucose hydrolases with differing catalytic activities. J. Biol. Chem. **273:**16021–16026.
8. **Edwards, K. A., M. Demsky, R. A. Montague, N. Weymouth, and D. P. Kiehart.** 1997. GFP-moesin illuminates actin cytoskeleton dynamics in living tissue and demonstrates cell shape changes during morphogenesis in *Drosophila*. Dev. Biol. **191:**103–117.
9. **Florin, I., and M. Thelestam.** 1981. Intoxication of cultured human lung fibroblasts with *Clostridium difficile* toxin. Infect. Immun. **33:**67–74.
10. **Florin, I., and M. Thelestam.** 1986. Lysosomal involvement in cellular intoxication with *Clostridium difficile* toxin B. Microb. Pathog. **1:**373–385.
11. **Gauthier-Rouvière, C., et al.** 1998. RhoG GTPase controls a pathway that independently activates Rac1 and Cdc42Hs. Mol. Biol. Cell **9:**1379–1394.
12. **Genth, H., et al.** 2006. Cellular stability of Rho-GTPases glucosylated by *Clostridium difficile* toxin B. FEBS Lett. **580:**3565–3569.
13. **George, W. L.** 1984. Antimicrobial agent associated colitis and diarrhea: historical background and clinical aspects. Rev. Infect. Dis. **6**(Suppl.)**:**208–213.
14. **Gerhard, R., et al.** 2005. *Clostridium difficile* toxin A induces expression of the stress-induced early gene product RhoB. J. Biol. Chem. **280:**1499–1505.
15. **Heap, J. T., et al.** 2010. The ClosTron: mutagenesis in *Clostridium* refined and streamlined. J. Microbiol. Methods **80:**49–55.
16. **Hidalgo, I. J., T. J. Raub, and R. T. Borchardt.** 1989. Characterization of the human colon carcinoma cell line (Caco-2) as a model system for intestinal epithelial permeability. Gastroenterology **96:**736–749.
17. **Huelsenbeck, J., et al.** 2007. Difference in the cytotoxic effects of toxin B from *Clostridium difficile* strain VPI 10463 and toxin B from variant *Clostridium difficile* strain 1470. Infect. Immun. **75:**801–809.
18. **Janoir, C., S. Péchiné, C. Grosdidier, and A. Collignon.** 2007. Cwp84, a surface-associated protein of *Clostridium difficile*, is a cysteine protease with degrading activity on extracellular matrix proteins. J. Bacteriol. **189:**7174–7180.
19. **Johal, S. S., K. Solomon, S. Dodson, S. P. Borriello, and Y. R. Mahida.** 2004. Differential effects of varying concentrations of *Clostridium difficile* toxin A on epithelial barrier function and expression of cytokines. J. Infect. Dis. **189:**2110–2119.
20. **Just, I., and R. Gerhard.** 2004. Large clostridial cytotoxins. Rev. Physiol. Biochem. Pharmacol. **152:**23–47.
21. **Karjalainen, T., et al.** 2001. Molecular and genomic analysis of genes encoding surface-anchored proteins from *Clostridium difficile*. Infect. Immun. **69:**3442–3446.
22. **Kato, H., et al.** 2010. Typing of *Clostridium difficile* isolates endemic in Japan by sequencing of *slpA* and its application to direct typing. J. Med. Microbiol. **59:**556–562.
23. **Kim, H., S. H. Rhee, C. Pothoulakis, and J. T. LaMont.** 2009. *Clostridium difficile* toxin A binds colonocyte Src causing dephosphorylation of focal adhesion kinase and paxillin. Exp. Cell Res. **315:**3336–3344.
24. **Kirby, J. M., et al.** 2009. Cwp84, a surface-associated cysteine protease, plays a role in the maturation of the surface layer of *Clostridium difficile*. J. Biol. Chem. **284:**34666–34673.
25. **Kreitman, R. J., and I. Pastan.** 1995. Importance of the glutamate residue of KDEL in increasing the cytotoxicity of *Pseudomonas* exotoxin derivatives and for increased binding to the KDEL receptor. Biochem. J. **307:**29–37.
26. **Kuehne, S. A., et al.** 2010. The role of toxin A and toxin B in *Clostridium difficile* infection. Nature **467:**711–713.
27. **Lencer, W. I., et al.** 1995. Targeting of cholera toxin and *Escherichia coli* heat labile toxin in polarized epithelia: role of COOH-terminal KDEL. J. Cell Biol. **131:**951–962.
28. **Luna, A., et al.** 2002. Regulation of protein transport from the Golgi complex to the endoplasmic reticulum by CDC42 and N-WASP. Mol. Biol. Cell **13:**866–879.

29. **Lyerly, D. M., K. E. Saum, D. K. MacDonald, and T. D. Wilkins.** 1985. Effects of *Clostridium difficile* toxins given intragastrically to animals. Infect. Immun. **47:**349–352.
30. **Lyras, D., et al.** 2009. Toxin B is essential for virulence of *Clostridium difficile*. Nature **458:**1176–1179.
31. **Matarrese, P., et al.** 2007. *Clostridium difficile* toxin B causes apoptosis in epithelial cells by thrilling mitochondria. Involvement of ATP-sensitive mitochondrial potassium channels. J. Biol. Chem. **282:**9029–9041.
32. **Meyer, G. K., et al.** 2007. *Clostridium difficile* toxins A and B directly stimulate human mast cells. Infect. Immun. **75:**3868–3876.
33. **Na, X., H. Kim, M. P. Moyer, C. Pothoulakis, and J. T. LaMont.** 2008. gp96 is a human colonocyte plasma membrane binding protein for *Clostridium difficile* toxin A. Infect. Immun. **76:**2862–2871.
34. **Nam, H. J., et al.** 2010. *Clostridium difficile* toxin A decreases acetylation of tubulin, leading to microtubule depolymerization through activation of histone deacetylase 6, and this mediates acute inflammation. J. Biol. Chem. **285:**32888–32896.
35. **Nusrat, A., et al.** 2001. *Clostridium difficile* toxins disrupt epithelial barrier function by altering membrane microdomain localization of tight junction proteins. Infect. Immun. **69:**1329–1336.
36. **Pothoulakis, C., and T. Lamont.** 2001. Microbes and microbial toxins: paradigms for microbial-mucosal interactions. II. The integrated response of the intestine to *Clostridium difficile* toxins. Am. J. Physiol. Gastrointest. Liver Physiol. **280:**G178–G183.
37. **Salari, M. H., N. Badami, N. Sadeghifard, and F. Amin Harati.** 2008. Investigation of various tissue culture monolayers sensitivity in detection of *Clostridium difficile* toxin. Iranian J. Publ. Health **37:**99–102.
38. **Sebaihia, M., et al.** 2006. The multidrug-resistant human pathogen *Clostridium difficile* has a highly mobile, mosaic genome. Nat. Genet. **38:**779–786.
39. **Siffert, J. C., et al.** 1993. Effects of *Clostridium difficile* toxin B on human monocytes and macrophages: possible relationship with cytoskeletal rearrangement. Infect. Immun. **61:**1082–1090.
40. **von Eichel-Streiber, C., P. Boquet, M. Sauerborn, and M. Thelestam.** 1996. Large clostridial cytotoxins—a family of glycosyltransferases modifying small GTP-binding proteins. Trends Microbiol. **4:**375–382.
41. **Voth, D. E., and J. D. Ballard.** 2005. *Clostridium difficile* toxins: mechanism of action and role in disease. Clin. Microbiol. Rev. **18:**247–263.
42. **Waligora, A. J., et al.** 2001. Characterization of a cell surface protein of *Clostridium difficile* with adhesive properties. Infect. Immun. **69:**2144–2153.
43. **Wrzeszczynski, K. O., and B. Rost.** 2004. Annotating proteins from endoplasmic reticulum and Golgi apparatus in eukaryotic proteomes. Cell. Mol. Life Sci. **61:**1341–1353.

Editor: J. B. Bliska